A lightweight, low-power electroadhesive clutch and spring for exoskeleton actuation

Stuart Diller[1], Carmel Majidi[1,2], and Steven H. Collins[1,2,*]

***Abstract*—Clutches can be used to enhance the functionality of springs or actuators in robotic devices. Here we describe a lightweight, low-power clutch used to control spring engagement in an ankle exoskeleton. The clutch is based on electrostatic adhesion between thin electrode sheets coated with a dielectric material. Each electrode pair weighs 1.5 g, bears up to 100 N, and changes states in less than 30 ms. We placed clutches in series with elastomer springs to allow control of spring engagement, and placed several clutched springs in parallel to discretely adjust stiffness. By engaging different numbers of springs, the system produced six different levels of stiffness. Force at peak displacement ranged from 14 to 501 N, and the device returned 95% of stored mechanical energy. Each clutched spring element weighed 26 g. We attached one clutched spring to an ankle exoskeleton and used it to engage the spring only while the foot was on the ground during 150 consecutive walking steps. Peak torque was 7.3 N·m on an average step, and the device consumed 0.6 mW of electricity. Compared to other electrically-controllable clutches, this approach results in three times higher torque density and two orders of magnitude lower power consumption per unit torque. We anticipate this technology will be incorporated into exoskeletons that tune stiffness online and into new actuator designs that utilize many lightweight, low-power clutches acting in concert.**

I. Introduction

Clutching has many uses in robotic systems, particularly in legged robotics. Clutches can disengage non-backdriveable geared motors to allow passive joint movement [1] or engage springs to allow force development with reduced, or zero [2], energy cost. Clutches can be used in hybrid actuation schemes where springs or actuators are engaged individually, in parallel, or in series for improved performance [3, 4]. These approaches can lead to lower energy use in bipedal robots [5, 6], lower-limb exoskeletons [7–9], and lower-limb prostheses [10, 11], and suggest other devices that could assist gait [12, 13].

Many types of clutches have been used in robotic devices. Electromagnetic clutches are a common choice [11, 14], featuring fast activation and moderate torque density, but also requiring continuous electrical power to stay active. Magnetorheological clutches can produce large torques without gearing [15–18], but are heavy and require continuous electrical power to remain active. Mechanical latches have high torque density and require no energy to stay active [2, 3, 5] but typically can only engage or disengage under special conditions particular to one application. Lightweight, low-power and electrically controllable clutches would allow higher performance in existing device designs and would enable new types of devices that employ many clutches.

Electrostatics present an alternative means of clutching with strong potential. Electrostatic force can be developed by applying a voltage to a pair of electrodes separated by an insulating dielectric layer. Charge can develop quickly, enabling electrical control of adhesion. Once charge is developed, power consumption is typically very low, arising only from leakage through the insulator. Very little electrode material is required to hold the charge, making lightweight electrodes possible. Many wall-climbing robots have used electrostatics to adhere to insulating substrates [19–24], using low power but typically requiring voltages too high for standard electronic components. Some of the adhesion in these systems is due to the inherent adhesion of the tacky polymers used as insulators, which causes the electrodes to remain adhered even once the voltage is removed [25, 26]. This makes them less desirable for clutching, where an automatic release would be advantageous.

Clutching using electrostatic force without tacky polymers has been demonstrated in robotics applications, but its effectiveness has been hindered by space charge. Space charge occurs when charge carriers are electrically forced into the surface of the dielectric and become trapped. This can attract charge to the electrode surfaces after the applied voltage is removed, causing the clutch to continue transmitting force [27, 28]. Residual forces can constitute a large portion of the holding force of the clutch, and can persist for long periods of time. Space charge may be more prevalent at high voltages, and can depend strongly on the materials that are exposed to the high electrical fields. Electroadhesive clutches that avoid both tackiness and space charge could match or exceed the controllability of electromagnetic clutches.

Our first goal in this study was to develop a general-purpose clutch that realizes the potential of electrostatic adhesion to achieve low mass, low power consumption, and high responsiveness. Our second goal was to characterize the electrical and physical performance of the device. Our third goal was to demonstrate an application to ankle exoskeletons, which we expected to illustrate potential uses and allow evaluation of clutch performance in a robotic system.

II. Methods

We created an electrostatic clutch comprised of flexible conductive electrodes coated with a high-dielectric insulator with no inherent adhesion. We placed the clutch in series

Based upon work supported by the National Science Foundation under Grant No. IIS-1355716 and by the John and Claire Bertucci Fellowship.

[1]Dept. Mechanical Engineering, Carnegie Mellon University, USA.
[2]Robotics Institute, Carnegie Mellon University, USA.
*Corresponding author: S. H. Collins., 5000 Forbes Ave., Pittsburgh, PA 15213, USA. Email: stevecollins@cmu.edu

with a polymer spring and performed tests of clutching force, resiliency, time to engage and disengage, and electrical power consumption. We placed several clutched springs in parallel and performed tests of stiffness selection. Finally, we incorporated the electrostatic clutch and spring into an ankle exoskeleton and collected data during normal walking.

We experimented with several materials as electrodes and force transmission components, including aluminum-sputtered BOPET (Bi-axially Oriented Polyethylene Terephthalate) film (Nielsen Enterprises, Kent, WA) with 25 μm thickness and aluminum foil with 50 μm thickness. The insulating dielectric was created by depositing a 25 μm layer of an uncured polymer-ceramic composite (Luxprint, Dupont Microcircuit Materials, Research Triangle Park, NC) containing barium titanate and titanium dioxide on one or both electrodes using a thin film applicator. The polymer was cured to a thickness of 10 μm in a ventilated oven at 140° C for 45 minutes. If only one of the two electrodes was to be coated, another 25 μm layer was applied and cured to create a final dielectric thickness of approximately 20 μm. The decrease in polymer thickness during curing occurred because a significant amount of solvent evaporated from the original mixture.

The electrodes were attached to the primed surface of carbon fiber shims using a polyacrylate adhesive (VHB, 3M, Maplewood, MN) (Fig. 1). Rubber bands were used as tensioners, fitting into slots cut in the carbon fiber. The energy storing spring was natural gum rubber (McMaster-Carr, Aurora, OH), with a width of 80 mm, a thickness of 1.6 mm, and a length of 27 mm. The spring was attached to carbon fiber shims using cyanoacrylate glue. Silver particle-based conductive epoxy (MG Chemicals, Burlington, Ontario, Canada) was used to make an electrical contact between ring terminal leads and the conductive electrode surface. A stretchable conductive fabric lead (Medtex P-130, Shieldex, Palmyra, New York) spanned the natural rubber spring. The alignment springs on each clutch plate were attached via slots to the other clutch plate, such that the dielectric coating was always separating the conductive surfaces. The tensioners maintained device alignment and kept the two sides of the electrostatic clutch in contact to ensure fast and reliable engagement during activation.

The desired spring stiffness and clutch force were calculated based on the torque requirements of a prior elastic exoskeleton [2]. The clutch was designed to operate with an overlapping surface area of 80 cm^2. The combined thickness of the clutch plates was 75 μm, while the clutched-spring device had a total thickness of 2.5 mm. The total width of the clutched spring device was 10 cm, and the device was 30 cm long. The mass of the clutch electrodes and dielectric was 1.5 g. Adding the carbon fiber, leads, and adhesive brought the total clutch mass to 11.2 g. Finally, adding the spring and two more carbon fiber bars brought the mass of the full clutched spring to 26 g.

Force-displacement testing of the clutched spring was conducted with a materials testing machine (Instron 5969, Instron, Norwood, MA). The clutched spring was strained at a rate of 30 mm·min^{-1} in both activated and unactivated states, to a spring strain of 100%. The force displacement curves were

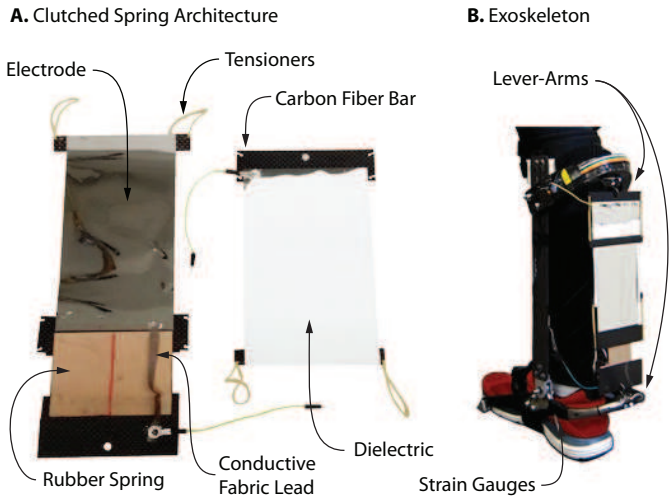

Fig. 1. Clutched spring components and construction. a) The clutch develops force when a voltage is applied across the electrodes, which are separated by a dielectric insulator. b) The clutch is mounted in series with a rubber spring on the ankle exoskeleton.

fitted to the Mooney-Rivlin model

$$\sigma_{eng} = (2C_1 + 2C_2\lambda^{-1})(\lambda - \lambda^{-2}) \quad (1)$$

where σ_{eng} is the engineering stress, λ is the spring stretch, and $2C_1$ and $2C_2$ are the coefficients obtained by fitting. The efficiency was calculated by numerically integrating the loading and unloading curves, then dividing the work of unloading by the work of loading. Two clutched springs were tested, three times each. Selective stiffness behavior was demonstrated with five clutched springs in parallel by activating various combinations before each test.

Release time was measured by turning off the clutch after the clutched spring had been loaded by a materials testing machine. The clutched spring was engaged and loaded to 50 N, and a microcontroller (Arduino Uno) shorted the clutch electrodes while simultaneously sending a signal to the digital input of the materials testing machine. The materials testing machine recorded the instant at which the digital input was received, indicating the time at which the clutch was deactivated. The clutched spring release time was defined as the 90% fall time, relative to the steady state force value after release. The materials testing machine digital input was observed to have a 12 ms average delay between the real clutch deactivation time and its recorded value. This delay was added to the measured data to produce the reported value. One BOPET electrode clutch was tested 4 times, and two aluminum electrode clutches were tested a total of 8 times.

The engage time was determined by comparing a 'dynamic engage' test, during which voltage was applied to the clutch while displacing the clutched spring, to the baseline force-displacement curve. The amount of extension undergone before the clutch was fully engaged was determined by shifting the reference force-displacement curve until the force profile in a 1 mm span coincided with an equivalent length segment of the dynamic engage curve. This span was chosen to be well

past the transient region of the dynamic engage curve, at least 2 mm from the extension at clutch engagement. The amount of shift corresponded to an extension value, which we equated to the amount of slip in the clutch during the time after the voltage was applied and before the clutch was fully engaged. Because the test took place at constant velocity, we correlated the amount of slip extension to a time value, and called this value the time to fully engage the clutch.

In order to determine the reference force displacement curve for engage time testing, the clutch was engaged for three seconds to ensure full engagement and then stretched at a displacement rate of 600 mm·min^{-1}. This procedure was performed three times, and the curves from the final two tests were averaged to produce a final curve. The 'dynamic engage' test was performed by initiating an extension velocity of 600 mm·min^{-1} while the clutch was deactivated. Once the peak velocity was reached, the microcontroller engaged the clutch while simultaneously signaling the digital input of the materials tester. The materials testing machine recorded the time when the digital input was received. The data was zero-phase digitally filtered with a 20 Hz low-pass second order filter. The zero-phase filter did not introduce a delay because the filtering was performed in both directions. The measurement delay of 12 ms was also added to the measured engage time values to produce the reported values. One BOPET electrode clutch was tested 4 times, and one aluminum electrode clutch was tested 3 times. The clutches used for engage and release timing tests had both electrodes coated.

The capacitance and power consumption of the clutches were determined by measuring current during charging and maintenance. A 330 kΩ shunt resistor was placed in series with the clutch, and the current was determined by measuring the voltage drop across the resistor with two high impedance voltage dividers. The capacitor was considered to be charging until the current was below 5% of the difference between the peak current value and the final leakage current value. The current was numerically integrated during charging to quantify the electrical charge stored on the electrodes. The capacitance was then calculated as

$$C = \frac{Q}{V} \tag{2}$$

where Q is the total charge and V is the applied voltage. We tested the accuracy of this procedure on commercial capacitors, and found values within 10% of the manufacturer-specified capacitance, which we separately confirmed using an LCR-meter (BK Precision 889B, Yorba Linda, CA). Using this method, capacitance and leakage current were calculated from 20 tests performed on 5 BOPET clutches.

Using measured values of the capacitance and the steady state leakage current of the clutch, the power consumption for the walking application was calculated as

$$P = I_{\text{leak}} \cdot V \cdot D + \frac{1}{2} \cdot C \cdot V^2 \cdot f \tag{3}$$

where I_{leak} is the leakage current, D is the fraction of time the clutch is on during walking, C is the capacitance of the clutch, and f is the frequency of activation.

The clutched spring was connected to the lever arms of the exoskeleton using eye hooks. The clutch used on the exoskeleton contained one coated and one uncoated BOPET electrode. The lower lever arm of the exoskeleton was instrumented with 4 strain gages, creating a full Wheatstone bridge that was calibrated to measure the torque acting on the lever arm [29]. The attachment point on the lower lever arm was a distance of 0.15 m from the exoskeleton ankle joint. An encoder was attached at the ankle joint to measure the angle of the foot relative to the shank. This signal was differentiated in software to determine the ankle velocity. The strain gages and encoder were connected to a real-time control hardware system (DS1103, dSPACE, Wixom, MI).

Clutch control signals were generated by the digital outputs of the control system. These signals activated Darlington Pair transistors, which in turn controlled high-voltage relays powered at 1.9 V. The outputs of the high-voltage relays were connected to the leads of the clutch, such that the electrode was either at high voltage, at ground voltage, or floating. The uncoated electrode was always connected to ground. A high-voltage power supply (Model PS375, Stanford Research Systems, Sunnyvale, CA) provided 240 V DC. A 330 kΩ resistor was placed in series with the clutch to keep the instantaneous current draw below the power supply's limit. Control commands were updated at a frequency of 500 Hz.

The clutch was controlled by a state machine. At maximum plantarflexion during early stance, the controller recorded the ankle angle and activated the clutch. The clutch then transmitted force as the spring stretched and recoiled during the stance phase. Once the recorded ankle angle was reached during late stance, indicating that the slack length of the spring had been reached, the clutch was deactivated to allow free rotation of the ankle during swing. During clutch deactivation, the electrode was switched between high and ground at 200 Hz for 50 ms, to facilitate clutch release based on a strategy previously used in electro-adhesion [28]. As a result, the spring on the exoskeleton engaged just after the foot contacted the ground, and disengaged as the foot left the ground.

Walking tests were conducted on a treadmill at 1.25 m·s^{-1} with one subject. Spring stiffness was reduced by decreasing the width from 80 mm to 45 mm because the original stiffness produced higher forces during walking than the clutch was designed to hold. 150 consecutive strides were taken during which the clutch performed as desired. Data was divided into individual strides, beginning with exoskeleton-side heel strike. Performance characteristics, including torque, power, efficiency, work, and stiffness were calculated for each step, then averaged. Power was calculated by multiplying instantaneous ankle joint velocity and torque. Negative work was calculated by integrating the torque-angle plot from the time that the clutch engaged to the time when the spring was maximally stretched. Positive work was calculated by integrating the torque-angle plot from the time of maximum stretch to the time the clutch disengaged. Efficiency was calculated as

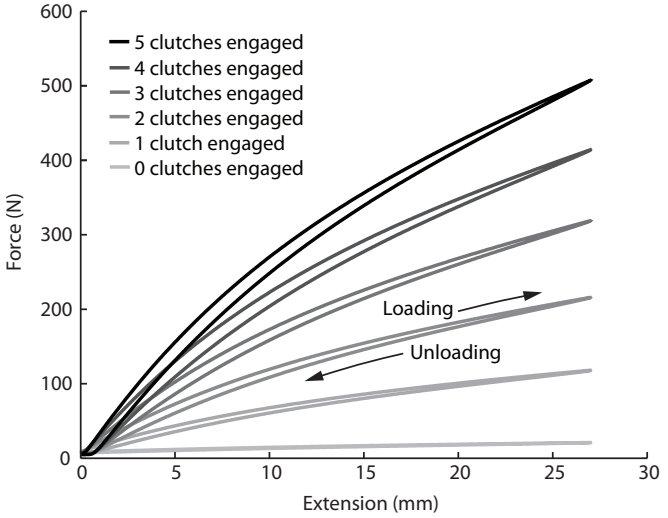

Fig. 2. Force-displacement curves for five clutched springs in parallel. Placing multiple clutched springs in parallel allows the overall device stiffness to be selected each cycle. The maximum device stiffness is 36 times higher than the minimum device stiffness.

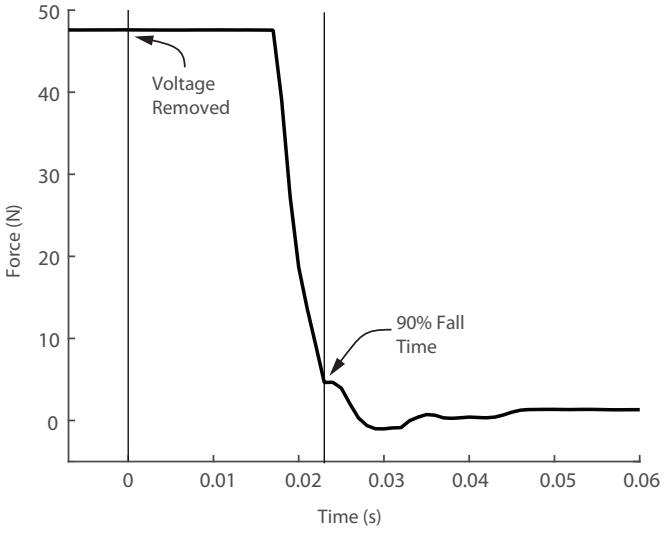

Fig. 3. Clutch release curve for a typical trial. The clutch does not release for about 20 ms before the force rapidly decreases and oscillates about the tensioner equilibrium force.

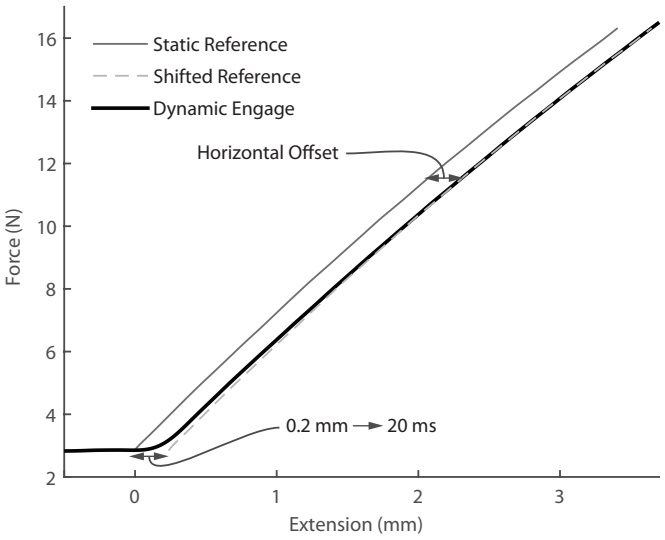

Fig. 4. Clutch engage curve for a typical trial. The static extension curve is shifted until the latter part of the curve coincides with the dynamic engage curve. The magnitude of the extension shift corresponds to the engage time.

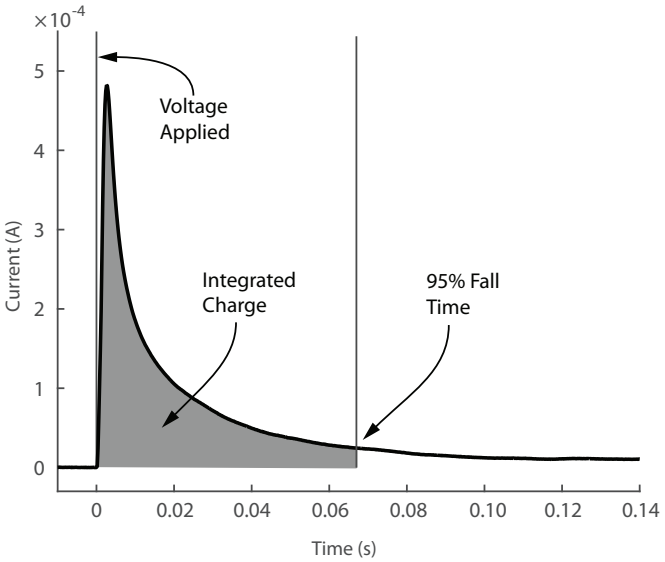

Fig. 5. Clutch charging data from a typical trial. Current peaks at about 5 ms, followed by an exponential decay characteristic of charging capacitors. The charge accumulated in the clutch is calculated by numerically integrating the current until it is within 5% of the leakage current.

the absolute value of positive work divided by negative work. Linearized exoskeleton stiffness was calculated by dividing the maximum torque by the maximum ankle angle.

III. Results

The modulus of elasticity of the clutched spring in its activated state was 238 ± 1 kPa (mean ± st. dev.). The full stress-strain behavior of the clutch-spring device was well described by the Mooney-Rivlin model, for which the coefficients were $2C_1$ = 314 kPa and $2C_2$ = 275 kPa, and the average RMS error of the fit was 1.1 kPa. The efficiency of the clutch-spring device was 94.7 ± 0.1 %. The average force reached at 100% spring strain was 100.1 ± 0.1 N (Fig. 2). Five clutched springs placed in parallel produced a peak force of 501 N with all clutches engaged and a peak force of 14 N with no clutches engaged, or a factor of 36 change in stiffness. Clutch release time was 29.7 ± 15.9 ms for the Mylar electrodes, and 23.6 ± 6.5 ms for the aluminum electrodes. Clutch engage time was 29.5 ± 12.0 ms for the Mylar electrodes, and 28.7 ± 5.0 ms for the aluminum electrodes.

The average capacitance of the Mylar electrode clutches was 21.8 ± 5.3 nF. The average leakage current was 310 ± 90 nA. The average charging time under no load was 111 ± 58 ms.

The maximum torque exerted by the clutched spring on the exoskeleton during walking was 7.37 ± 0.04 N·m. The linearized exoskeleton stiffness was 14.7 ± 0.9 N·m·rad^{-1}. The efficiency of the exoskeleton during walking was 81.9 ± 3.6%. The maximum instantaneous power was 25.6 ± 2.4 W dur-

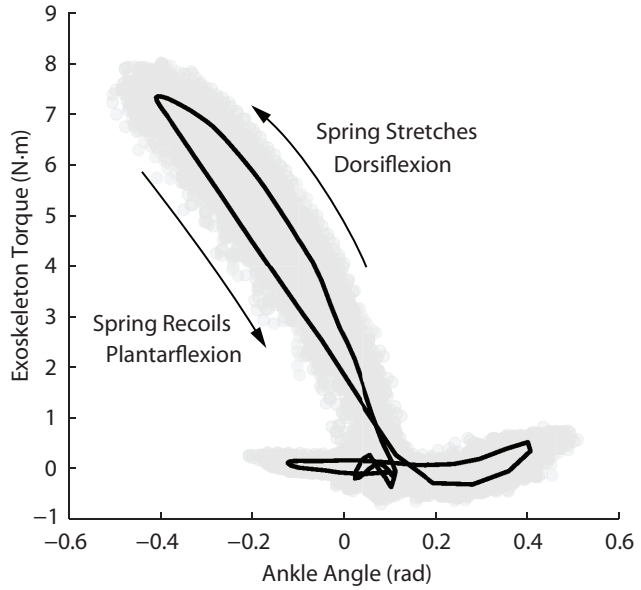

Fig. 6. Exoskeleton torque-angle curve during walking. The exoskeleton displays two distinct slopes, corresponding to the exoskeleton stiffnesses during the activated and unactivated clutch states. The steep slope occurs during stance and push-off, when the clutch is engaged. Very little torque is produced during leg swing, when the clutch is disengaged. More energy loss was observed during walking than in benchtop tests (Fig. 2), likely owing to acceleration of the ankle lever arm of the exoskeleton during plantarflexion.

ing push-off. The clutched spring performed 2.61 $\pm$ 0.33 J of negative work and 2.14 $\pm$ 0.29 J of positive work on each step. The fraction of time the clutch was activated during walking was D = 0.524, and the stride frequency was 0.873 Hz. This resulted in a power loss from leakage current of 0.05 mW, and an average total electrical power consumption of 0.59 $\pm$ 0.14 mW.

IV. Discussion

Our goal was to design and characterize a lightweight, low-power electroadhesive clutch, and to demonstrate its use in selectable stiffness and exoskeleton applications. The electroadhesive clutch tested here had a total mass of 11 g, transmitted 100 N of force, and consumed only 0.6 mW of electricity during walking. This is a three-fold improvement in weight and a factor of 340 improvement in power consumption compared to the best conventional clutches used in similar applications. Placing several clutch-spring elements in parallel allowed stiffness selection, enabling a 36-fold increase in stiffness. The electroadhesive clutch-spring device controllably and reliably produced torque on the ankle exoskeleton during walking, and separate testing showed that the clutch fully engages and releases in less than 30 ms. This technology can be used in high-performance exoskeletons, prostheses, and walking robots, allowing the use of many separately-controlled clutches while achieving low mass and power consumption.

Characterization of the clutch and spring demonstrated predictable and reliable behavior. The stress-strain behavior of the clutched rubber spring was repeatable across samples and tests, and was well-predicted by the Mooney-Rivlin model. The efficiency of the rubber spring was almost 95%, comparable to metal coil springs. The clutch displayed no distinguishable slipping, evident in force-displacement curves and in the match between clutched spring efficiency and the efficiency of the spring measured without the clutch.

Stiffness was controllably changed by selectively engaging a subset of clutched springs acting in parallel. A stiffness ratio of 36 was demonstrated, with fast activation and deactivation and very low power consumption. Improved resolution could be achieved using springs of differing stiffness, increasing exponentially with the number of clutched springs. For example, five springs with power-of-two ratios in stiffness would yield 32 evenly distributed stiffnesses. Using this approach with electroadhesive clutches could enhance performance and add functionality in applications using rigidity tuning devices [30, 31] or variable stiffness actuators [32–35].

Measurements of clutch release time demonstrated fast state changes, and suggest that faster release may be possible. Upon shorting of the electrodes, the clutch took about 30 ms to fully disengage. For the first 20 ms, no reduction in holding force was observed (Fig. 3). This suggests that more charge was applied than would have been necessary to prevent slipping, resulting in a delay between the onset of discharge and the release of the electrodes. Faster release may therefore be possible by regulating voltage to be slightly above that required to achieve instantaneous holding force requirements.

During release tests, there were some oscillations as the force approached zero. Some of this high-frequency behavior may have to do with the physical dynamics of the clutched spring. An analysis of a mass-spring-damper model of the system suggests that the viscosity of the tensioning springs could be accountable for the force rise and decay during this extremely rapid movement. The clutch plate and spring travel at high speed before reaching the rest length of the spring, at which point they visibly and loudly vibrate, possibly causing small oscillatory loads. This phenomenon is unlikely to occur in typical applications, where it would be undesirable to release the spring under load and lose stored strain energy.

Clutches engaged quickly during dynamic engage tests. Upon application of high voltage, the clutch engaged within about 30 ms, with some slipping occurring before full engagement (Fig. 4). During engagement, the electrodes move to eliminate the air gap and physically conform. Engage time might therefore be improved by adjusting the clutch structure, geometry, and tensioning springs. Electrical dynamics may also have influenced engage time, suggesting faster engagement if the clutch were charged more quickly by a capacitor.

Clutch charging closely resembled theoretical capacitor charging curves, with a few small differences. The current initially increased for about 5 ms, likely relating to the closing of the air gap between electrodes and a corresponding increase in capacitance. The average charge time was 111 ms, about four times longer than the measured engage time. However, most of the charge is accumulated early in the charging curve, so the charge required to resist slipping is apparently reached before the plates are fully charged. The average leakage current was

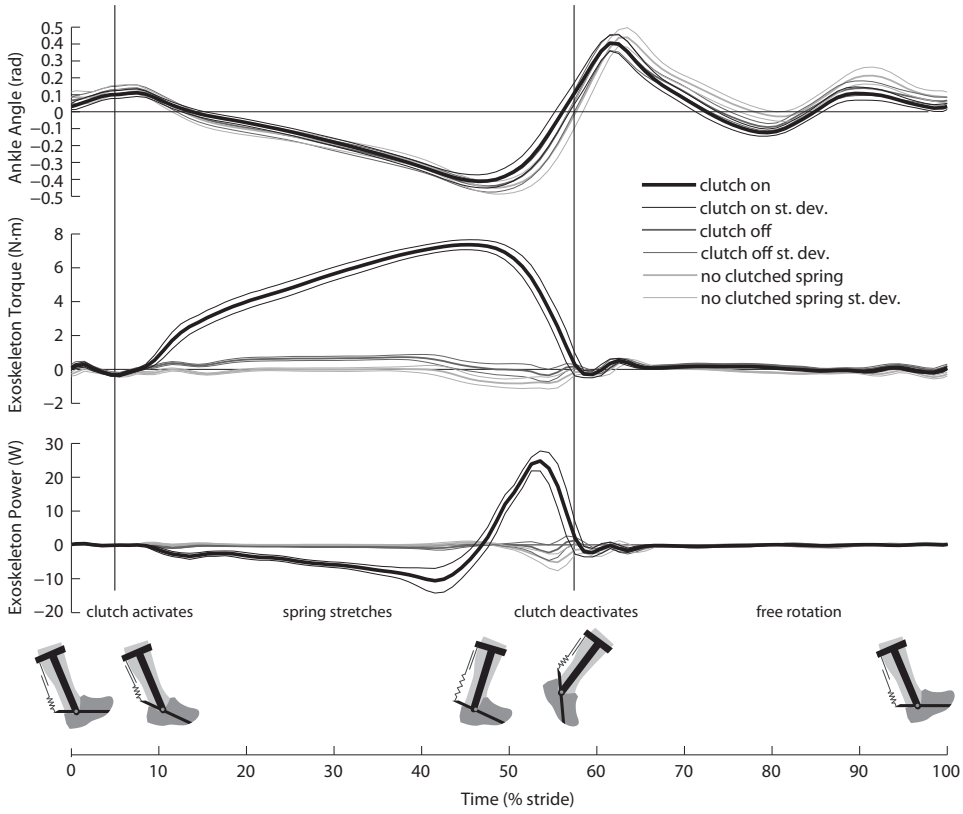

Fig. 7. Ankle angle, measured torque, and exoskeleton power during the gait cycle. The "clutch on" data is from walking with the clutch activated during stance, between the vertical lines. The "clutch off" data is from walking when the clutch was deactivated throughout the gait cycle. Positive torque in this data is produced only by the tensioning springs and motion artifact from the inertia of the lever arm. The "no clutched spring" data is from walking in the exoskeleton without any clutch attached to the spurs.

low (310 nA), meaning that if the clutch were engaged and disengaged at 1 Hz, such as during walking, initial charging would account for more than 90% of power consumption. The charging curve implies an interesting relationship between the physical adhesion of the plates and the clutch's electrical state, which we will investigate in future experiments.

One of the features enabling quick clutch release is the hard dielectric material used. Electrostatic components of wall-climbing robots typically embed electrodes into soft or tacky elastomers, and typically operate at voltages in the 1-5 kV range [19–24]. In these systems, much of the adhesion comes from the inherent adhesion of the elastomer. This means that the device will continue to adhere even when the voltage is removed, which can be useful in wall-climbing. Peeling mechanisms are used to break adhesion when desired. Inherent adhesion is detrimental in clutch applications, however, as it slows and complicates disengagement. The hard dielectric material used here has no inherent adhesion, enabling automatic disengagement when voltage is removed.

Thin, flexible electrodes were used to achieve extensive surface contact and high holding force despite the hard dielectric layer. This strategy has been used in prior electrostatic clutches [27, 28]. The present system combines this effect with the use of a high-permittivity dielectric material to achieve about the same force density as prior electrostatic clutches [27, 28], but with two to four times lower voltage and about ten times lower electrical power consumption. The barium titanate fluoropolymer composite exhibited a high dielectric constant compared to common insulators such as Mylar, Parylene or Kapton. This allowed more charge to accumulate per unit voltage, leading to a lower required voltage for a given geometry and holding force. In informal tests, we found that choice of dielectric material strongly influenced susceptibility to space charge, and that space charge seemed to begin accumulating at a distinct voltage threshold. The barium titanate composite was resistant to space charge at voltages up to 300 V, allowing operation at 240 V without apparent space charge. Operation at this lower voltage helped avoid the undesired adhesion caused by space charge upon voltage removal. By eliminating both tackiness and space charge, the clutch achieved fast, automatic release. This operating voltage also allows use of standard electronics hardware. A mobile version of the exoskeleton could therefore use compact electronics powered by a small battery and transformer or by a high-voltage static charger [36].

The clutched-spring exoskeleton performed well during walking. The clutch consistently engaged the spring during the stance phase, and disengaged during swing to allow free rotation of the ankle (Fig. 7). No slipping or breakdown events were observed during 150 continuous steps of walking.

The observed variations in the torque vs stride curve are typical of natural step-to-step variations during walking. This result demonstrates that the electroadhesive clutch can operate reliably in a dynamic and challenging application.

During walking, small fluctuations in torque and power occurred at the transition to the swing phase. Fluctuations (Fig. 7, 60% stride) appear in all three conditions, including the no spring condition, and do not appear to be related to the clutch or spring. We attribute this to the inertia of the ankle lever, which likely bounces somewhat at the onset of swing.

The efficiency of the clutched spring appeared to be lower during walking than in benchtop tests, likely due to losses in accelerating exoskeleton components. Exoskeleton efficiency was 13% lower than the benchtop efficiency of the clutched spring, similar to differences observed with other passive-elastic exoskeletons [2]. Some of the positive work of the spring during plantarflexion was likely used to accelerate the ankle lever. During dorsiflexion the spring and ankle lever deflect slowly, but later during plantarflexion the ankle lever accelerates forwards and upwards rapidly. Torque measurements were made using strain gages near the cantilever point of the lever. The spring force that accelerated the distal mass of the lever was therefore not observed as positive work at the ankle joint, reducing the observed positive work and the measured efficiency. With larger spring forces this effect would be reduced, because energy used to accelerate the lever would remain constant while the total positive work would increase. Damping in the series spring could also account for some energy loss during walking. The unloading strain rate during plantarflexion is higher than we could produce with the materials testing machine, which could cause a transition into in a region with lower efficiency.

The electroadhesive clutch achieved significant improvements in mass and power consumption compared to other types of clutches. Such comparisons are imperfect, because electromagnetic and magnetorheological clutches are usually rotary, so we have based comparisons on estimates of the mass and power required to provide similar functionality.

High-performance electromagnetic clutches provide one point of comparison. The best reported performance for a similar application is found in [11], which describes a clutch in series with a spring in a lower-limb prosthesis. During the stance phase of walking the clutch held one end of the spring stationary, allowing it to passively produce torque. The clutch weighed 100 g and used 3.14 W to produce 0.75 N·m of torque, which was geared to 107 N·m. The mass of the spring, ball screw, pulleys, and other gearing hardware was 818 g, bringing the total mass for the clutched spring to 919 g. Comparable performance would be achieved by stacking electroadhesive clutched springs in parallel, adding a pair of electrodes to each spring, and doubling the spring thickness. This would produce 200 N of force for every 42.3 g clutched spring added. The lever arm in this system is analogous to the gearing hardware in the prosthesis, and has a mass of 130 g. This means the electroadhesive clutch system would produce 107 N·m of torque with about 281 g, or a third of the mass of the electromagnetic clutch system. The power consumption would be 4.2 mW, or 750 times lower. The electroadhesive clutch-spring system would also have the added benefit of discretely variable series stiffness.

Another point of comparison is high-performance magnetorheological clutch systems. The best reported performance is provided by [17]. This clutch weighed 4.5 kg, produced 75 N·m of torque without any gearing, and consumed at least 1 W of power (estimated from similar devices [15–18]). Comparable performance would be achieved by stacking electroadhesive clutches in parallel and adding another set of electrodes to each carbon fiber shim. The same torque would be produced with 32 g of clutches and 162 g total mass, corresponding to 30 times less mass. Power consumption would be 2.95 mW, a factor of 340 reduction. The magnetorheological clutch has the added benefit of controlled damping, which has not yet been demonstrated with this electroadhesive clutch.

The electroadhesive clutch even achieves a weight savings compared to passive clutches. Similar functionality is described by [2], which presents a passive ratchet and pawl clutch connected to a metal coil spring on an exoskeleton. The passive clutch and metal spring produce a torque of 36 N·m with a mass of 155 g. Comparable performance would be achieved with 50.9 g of electroadhesive clutches and rubber springs. This three-fold mass reduction comes with the advantage of electrically controlled engagement and selectable stiffness. These comparisons illustrate the potential for the electroadhesive clutch to achieve significant weight and power savings while offering the ability to quickly and controllably change stiffness without interrupting operation.

Despite its many advantages, the electroadhesive clutch has some potential disadvantages. Failure can occur because of dielectric breakdown, or a shorting of the electrodes through the insulating layer. This can cause the clutch to disengage, and can expend a significant amount of electrical energy. However, the use of thin electrodes leads to a self-cauterizing property, or the tendency of the electrode surface near the breakdown to be ablated. As a result, subsequent recharging of the electrode surfaces does not lead to recurring shorting, and the clutch almost always continues to function as it did before the breakdown. Operation at 240 V could also pose some risks, but very little energy is stored during operation, limiting the risk to humans. In the future, electrodes could be completely insulated by a dielectric layer, further reducing risk. Manufacturing of the dielectric-coated electrodes remains a challenge; only about 50% of the clutches we have produced worked consistently and without space charge. We have not yet characterized the fatigue properties of the device, which could limit its applicability in repetitive tasks such as walking.

The promising characteristics of this electroadhesive clutch suggest a variety of impactful applications. Clutched spring exoskeletons have been suggested for assistance at the knee and hip [12, 37, 38] as well as the ankle. Exoskeleton mass seems to strongly affect performance, making lightweight, low-power electroadhesive clutches an excellent option. Electroadhesive clutches could also replace heavier, energy-intensive compo-

nents in prostheses and robots. Finally, because of their exceptionally low mass and power requirements, electroadhesive clutches may enable actuator designs involving many clutches acting in concert.

V. Conclusions

The electroadhesive clutch presented here is lightweight, energy efficient and controllable. Combining electroadhesive clutch-spring elements in parallel created a versatile selectable-stiffness device. Clutched springs demonstrated reliable performance during walking tests with an ankle exoskeleton. This technology promises to enable the design of high-performance mobile wearable robots, including complex actuation schemes that incorporate many clutches, while meeting tight constraints on mass and energy use.

VI. Acknowledgments

The authors thank Kirby Ann Witte and Juanjuan Zhang for their contributions to exoskeleton construction and control software development.

[1] V. I. Babitsky and A. Shipilov, *Resonant robotic systems*. Berlin, Germany: Springer Science & Business Media, 2012.

[2] S. H. Collins, M. B. Wiggin, and G. S. Sawicki, "Reducing the energy cost of human walking using an unpowered exoskeleton," *Nature*, vol. 522, 2015.

[3] M. Plooij, "Review of locking devices used in robotics," *Rob. Autom. Mag.*, vol. 22, 2015.

[4] T. R. Hunt, C. J. Berthelette, and M. B. Popovic, "Linear one-to-many (otm) system," in *Proc. Int. Conf. Tech. Pract. Rob. App.*, 2013, pp. 1–6.

[5] S. H. Collins *et al.*, "Efficient bipedal robots based on passive-dynamic walkers," *Science*, vol. 307, pp. 1082–1085, 2005.

[6] H. Yali *et al.*, "Hopping movement simulation of elastic actuator," in *Proc. Int. Conf. Mech. Aut.*, 2015, pp. 2203–2208.

[7] G. Elliott *et al.*, "The biomechanics and energetics of human running using an elastic knee exoskeleton," in *Proc. Int. Conf. Rehab. Rob.*, 2013, pp. 1–6.

[8] K. Shamaei *et al.*, "Design and evaluation of a quasi-passive knee exoskeleton for investigation of motor adaptation in lower extremity joints," *Trans. Biomed. Eng.*, vol. 61, pp. 1809–1821, 2014.

[9] C. Zhang *et al.*, "Design of a quasi-passive 3 dofs ankle-foot wearable rehabilitation orthosis," *Bio-Med. Mater. Eng.*, vol. 26, pp. 647–654, 2015.

[10] S. H. Collins and A. D. Kuo, "Recycling energy to restore impaired ankle function during human walking," *PLoS: ONE*, vol. 5, p. e9307, 2010.

[11] E. Rouse, L. Mooney, and H. Herr, "Clutchable series-elastic actuator: Implications for prosthetic knee design," *Int. J. Rob. Res.*, pp. 1–15, 2014.

[12] K. Endo, D. Paluska, and H. Herr, "A quasi-passive model of human leg function in level-ground walking," in *Proc. Int. Conf. Intel. Rob. Sys.*, 2006, pp. 4935–4939.

[13] M. P. Cortez and A. Forner-Cordero, "On the study of a clutch device for exoskeletons and robot joints: Energetic efficiency study and mechanism concept," in *Proc. Int. Symp. Dyn. Prob. Mech.*, 2015.

[14] Y. Sugahara *et al.*, "Design of a battery-powered multi-purpose bipedal locomotor with parallel mechanism," in *Proc. Int. Conf. Intel. Rob. Sys.*, 2002, pp. 2658–2663.

[15] D. M. Wang, Y. F. Hou, and Z. Z. Tian, "A novel high-torque magnetorheological brake with a water cooling method for heat dissipation," *Smart Mater. Struct.*, vol. 22, p. 025019, 2013.

[16] T. Saito and H. Ikeda, "Development of normally closed type of magnetorheological clutch and its application to safe torque control system of human-collaborative robot," *J. Intel. Mat. Syst. Str.*, vol. 18.12, pp. 1181–1185, 2007.

[17] A. S. Shafer and M. R. Kermani, "Design and validation of a magnetorheological clutch for practical control applications in human-friendly manipulation," in *Proc. Int. Conf. Rob. Autom.*, 2011, pp. 4266–4271.

[18] H. Bose, T. Gerlach, and J. Ehrlich, "Magnetorheological torque transmission devices with permanent magnets," *J. Phys: Conf. Series*, vol. 412, p. 012050, 2013.

[19] J. P. D. Tellez, J. Krahn, and C. Menon, "Characterization of electroadhesives for robotic applications," in *Proc. Int. Conf. Rob. Biomim.*, 2011, pp. 1867–1872.

[20] A. Takada *et al.*, "Design of electrostatic adhesion device using the flexible electrodes," in *Proc. Int. Symp. Micro-NanoMechatron. Hum. Sci.*, 2014, pp. 1–4.

[21] J. Krahn and C. Menon, "Electro-dry-adhesion," *Langmuir*, vol. 28, pp. 5438–5443, 2012.

[22] A. Chen, A. Charalambides, and S. Bergbreiter, "High strength, low voltage microfabricated electroadhesives on non-conductive surfaces," in *Sol.-State Sens. Act. Microsys. Workshop*, 2014.

[23] D. Ruffatto, J. Shah, and M. Spenko, "Increasing the adhesion force of electrostatic adhesives using optimized electrode geometry and a novel manufacturing process," *J. Electrostatics*, vol. 72, pp. 147–155, 2014.

[24] H. Prahlad *et al.*, "Electroadhesive robotswall climbing robots enabled by a novel, robust, and electrically controllable adhesion technology," in *Proc. Int. Conf. Rob. Autom.*, 2008, pp. 3028–3033.

[25] M. D. Bartlett, A. B. Croll, and A. J. Crosby, "Designing bioinspired adhesives for shear loading: From simple structures to complex patterns," *Adv. Fun. Mat.*, vol. 22, pp. 4985–4992, 2012.

[26] M. Bartlett, D. Michael, and A. J. Crosby, "High capacity, easy release adhesives from renewable materials," *Adv. Mat.*, vol. 26, pp. 3405–3409, 2014.

[27] D. Aukes *et al.*, "Design and testing of a selectively compliant underactuated hand," *Int. J. Rob. Res.*, pp. 1–15, 2014.

[28] M. E. Karagozler *et al.*, "Electrostatic latching for inter-module adhesion, power transfer, and communication in modular robots," in *Proc. Int. Conf. Intel. Rob. Sys.*, 2007, pp. 2779–2786.

[29] K. A. Witte *et al.*, "Design of two lightweight, high-bandwidth torque-controlled ankle exoskeletons," in *Proc. Int. Conf. Rob. Autom.*, 2015.

[30] W. Shan *et al.*, "Rigidity-tuning conductive elastomer," *Smart Mater. Struct.*, vol. 24, p. 065001, 2015.

[31] A. Balasubramanian, M. Standish, and C. J. Bettinger, "Microfluidic thermally activated materials for rapid control of macroscopic compliance," *Adv. Fun. Mat.*, vol. 24, pp. 4860–4866, 2014.

[32] R. Van Ham *et al.*, "Compliant actuator designs," *Rob. Autom. Mag.*, vol. 16, pp. 81–94, 2009.

[33] C. S. Haines *et al.*, "Artificial muscles from fishing line and sewing thread," *Science*, vol. 343, pp. 868–872, 2014.

[34] A. Jafari *et al.*, "A novel actuator with adjustable stiffness (awas)," in *Proc. Int. Conf. Intel. Rob. Sys.*, 2010, pp. 4201–4206.

[35] G. Mathijssen, D. Lefeber, and B. Vanderborght, "Variable recruitment of parallel elastic elements: Series-parallel elastic actuators (spea) with dephased mutilated gears," *Trans. Mechatr.*, vol. 20, pp. 594–602, 2015.

[36] A. Mujibiya, "Corona: Interactivity of body electrostatics in mobile scenarios using wearable high-voltage static charger," in *Proc. Int. Conf. Hum.-Comp. Interact. Mob. Dev. Serv.*, 2015, pp. 435–444.

[37] A. J. van den Bogert, "Exotendons for assistance of human locomotion," *BioMed. Eng. OnLine*, vol. 2, p. 17, 2003.

[38] W. van Dijk and H. V. der Kooij, "Xped2: A passive exoskeleton with artificial tendons," *Rob. Autom. Mag.*, vol. 21, pp. 56–61, 2014.